

Symbolic transfer entropy analysis of the dust interaction in the presence of wakefields in dusty plasmas

André Melzer* and André Schella

Institut für Physik, Ernst-Moritz-Arndt-Universität Greifswald, 17489 Greifswald, Germany

(Received 11 March 2014; published 24 April 2014)

The method of symbolic transfer entropy has been applied to analyze the behavior of charged-particle systems under the influence of an ion focus (wakefield) in a dusty plasma. Using long-run experiments under various plasma and trapping conditions, it is revealed from the transfer entropy that information is transported from the upper particle in an ion flow to the lower. The information transfer increases with smaller interparticle distance and with reduced height in the sheath. This can be consistently explained by the formation of the ion focus by an ion flow in the sheath. From the analysis of two-particle and many-particle systems, the symbolic entropy transfer can be judged as a reliable measure for information asymmetry, and hence interaction asymmetry, in dusty plasma systems.

DOI: [10.1103/PhysRevE.89.041103](https://doi.org/10.1103/PhysRevE.89.041103)

PACS number(s): 52.27.Lw, 02.50.-r, 05.45.Tp

Directed processes usually drive asymmetries in physical systems. An example is the formation of an ion focus (or wakefield) in particle-containing, “dusty,” plasmas with directed, streaming ions. Since dusty plasmas allow to measure the full dynamical properties of the individual particles on the kinetic level over long times, these systems are ideal to extract statistical information from the particles’ motion. Here, by exploiting techniques from information theory, namely, the (symbolic) transfer entropy, we will measure the asymmetry of the particle interaction due to the ion focus.

Dusty plasma usually consist of highly charged microspheres that acquire a (negative) charge due to the continuous inflow of plasma electrons and ions. Because of their high charge the dust-dust interaction is strongly coupled [1–3]. The spatial and temporal scales of the dust motion allow for a detailed observation by video microscopy [4] where the particle motion can be resolved on the microscopic dynamic level.

The particles are usually trapped in a region with streaming ions, such as the space charge sheath. There, downstream of the particles an ion focus or wakefield is formed [5–22]: The streaming ions are deflected in the electric field of the negatively charged particle and are scattered into a region downstream of the dust particle forming an enhanced positive charge, there. It has been found from theory, simulations, and experiments that the interaction between two dust particles at different heights in the sheath is not reciprocal, but asymmetric in that the downstream particle feels an attractive force due to the ion focus of the upstream particle, but the upstream particle is repelled from the downstream one [8–10,18,23–26]. Moreover, the wakefield of the upstream particle affects the charging properties of the downstream particle due to the modified ion streaming motion [27–29].

However, there has been no attempt yet to detect the asymmetry in the particle interaction from a statistical, probabilistic measure using the detailed microscopic dynamic information of the particles’ motion. Here we will apply the symbolic transfer entropy (STE) to determine driving

and responding particles from time series A_i and B_i of different particles in an ion stream. Transfer entropy has been used in various systems ranging from physiology to climate science [30–33] to detect influences, or even causality, between different agents. Hence, it is reasonable to try STE to detect dependencies in the wakefield interaction between dust particles. To reduce contributions of noise in the time series, the symbolic representation of the time series [34] has been proven successful for the analysis of transfer entropy [33]. In this STE, not the time series A_i , B_i themselves are used, but their symbolic representations determined from ordering the amplitude values of these time series.

Following Refs. [33,34], we start from a time series $A_i = \{a_i\}$ with the amplitude values a_i recorded at sampling instance i . Given an embedding dimension m and a delay ℓ the amplitude values are combined to $\{a(i), a(i + \ell), \dots, a(i + (m - 1)\ell)\}$, giving a sequence of length m for each instance i . These sequences are then sorted in ascending order $\{a(i + (k_{i1} - 1)\ell) \leq a[i + (k_{i2} - 1)\ell] \leq \dots \leq a[i + (k_{im} - 1)\ell]\}$. A symbol then denotes the order indices $\hat{a}_i \equiv (k_{i1}, k_{i2}, \dots, k_{im})$ thus mapping this sequence onto one of the possible $m!$ permutations of the numbers 1 to m reflecting the successive order of the amplitude values. This is done analogously for the time series $B_i = \{b_i\}$. From these symbols then the symbolic transfer entropy is defined as

$$T_{B \rightarrow A}^S = \sum_{\hat{a}_{i+1}, \hat{a}_i, \hat{b}_i} p(\hat{a}_{i+1}, \hat{a}_i, \hat{b}_i) \log \frac{p(\hat{a}_{i+1} | \hat{a}_i, \hat{b}_i)}{p(\hat{a}_{i+1} | \hat{a}_i)}, \quad (1)$$

that describes the information transfer from the time series B_i to A_i . Here $p(\hat{a}_{i+1}, \hat{a}_i, \hat{b}_i)$ is the joint probability of finding the symbols \hat{a}_{i+1} at instant $i + 1$ together with \hat{a}_i and \hat{b}_i at instant i . Further, $p(\hat{a}_{i+1} | \hat{a}_i, \hat{b}_i)$ is the conditional probability of finding the symbol \hat{a}_{i+1} at instant $i + 1$ under the condition that we have \hat{a}_i and \hat{b}_i at instant i . Equivalently, $p(\hat{a}_{i+1} | \hat{a}_i)$ is the conditional probability to find \hat{a}_{i+1} with \hat{a}_i given at instant i . This can be interpreted as the Shannon-like entropy that is found for finding \hat{a}_{i+1} at the instant $i + 1$ under the knowledge of both \hat{a}_i and \hat{b}_i at instant i tested against the consecution of \hat{a}_{i+1} from \hat{a}_i alone. This STE defines an asymmetric measure that describes the additional amount of information gained (or required) to represent the next observation \hat{a}_{i+1} from the

*melzer@physik.uni-greifswald.de

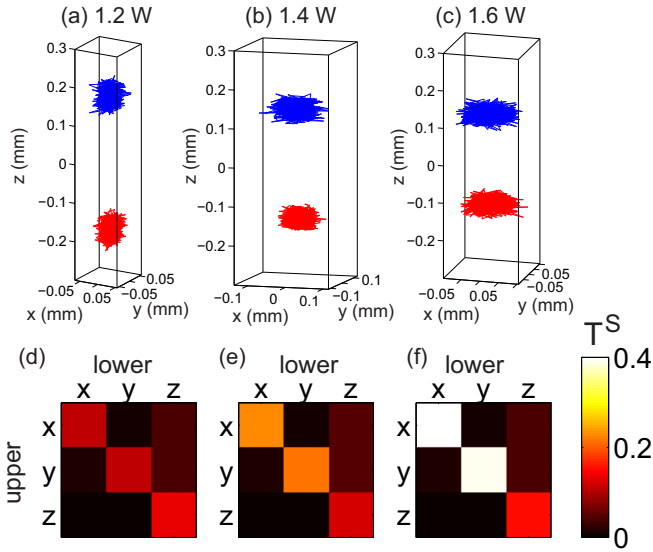


FIG. 1. (Color online) Particle trajectories of the two-particle system at discharge powers of (a) 1.2 W, (b) 1.4 W, and (c) 1.6 W at a gas pressure of 8 Pa. Directionality index T^S in false colors for the three situations at (d) 1.2, (e) 1.4, and (f) 1.6 W. The directionality index is calculated taking the x , y and z coordinate of the upper versus the coordinates of the lower particle.

previous observation \hat{a}_i and the input from \hat{b}_i . Hence, this quantifies the influence of B_i on A_i .

Using the analogous definition of the STE $T_{A \rightarrow B}^S$ from A_i to B_i , the directionality index of the STE can be defined as [33]

$$T^S = T_{A \rightarrow B}^S - T_{B \rightarrow A}^S, \quad (2)$$

where $T^S > 0$ when A is the driver and B is the responding system (analogously $T^S < 0$ for B being the driver and A responding). In order to test the asymmetry in the interaction between upstream and downstream dust particle in an ion flow we will calculate the directionality index T^S for time series A_i and B_i from the dust particle trajectories in a streaming plasma environment [35].

The experiments on the dust systems have been performed in a capacitively coupled radio-frequency ($f_{RF} = 13.56$ MHz) discharge in argon described in detail elsewhere [36–38]. Melamine-formaldehyde microspheres of $4.86 \mu\text{m}$ diameter are trapped inside a cubic glass box that provides a harmonic three-dimensional confinement for the particles [39]. The particle motion is followed in three dimensions using a stereoscopic camera setup [37], and time series of 20 000 to 100 000 frames at a frame rate of 100 Hz have been recorded. Gas pressures were varied between 4 and 8 Pa, and the rf power ranged between 0.8 W and 2.2 W.

We start with the simplest system of two trapped particles. Figure 1(a)–(c) shows the particle trajectories of the two-particle system at 8 Pa and different rf powers. The particles are vertically aligned as can be expected from the action of the ion focus. The particles just move under the influence of their thermal Brownian motion and their mutual (ion-focus mediated) interaction. The trajectories show similar behavior

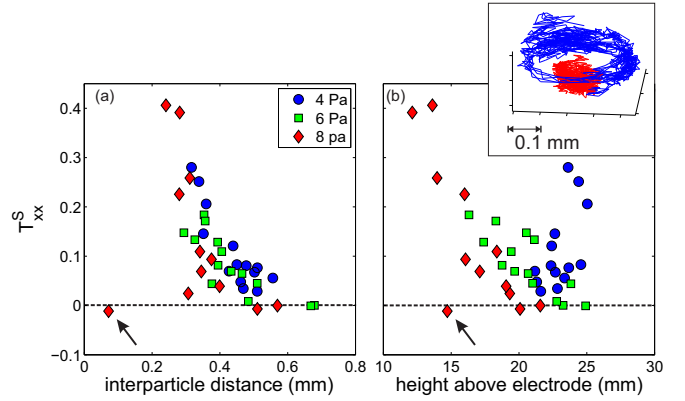


FIG. 2. (Color online) Directionality index T_{xx}^S for the x components of the upper and lower particle trajectory. In (a) T_{xx}^S is shown as a function of interparticle distance, whereas in (b) it is given as a function of height above the lower electrode. The particle trajectories of the outlier in (a) and (b), which is marked by the arrow, are shown as an inset.

in the three cases; only the vertical distance between the particles is reduced with increasing plasma power.

For these situations, the STE and the associated directionality indices have been calculated from Eqs. (2) and (1); see Fig. 1(d)–(f). There we have taken the x , y , and z coordinate of the particle trajectory of the upper particle as the time series A and those of the lower particle as time series B .

It can be seen that information transfer only occurs between the same coordinates x_{upr} versus x_{low} , y_{up} versus y_{low} , and z_{up} versus z_{low} . All other components are essentially zero. Further, the diagonal elements T_{xx}^S and T_{yy}^S are almost equal and increase with increasing plasma power from $T_{xx}^S \approx T_{yy}^S \approx 0.11$ at 1.2 W via $T_{xx}^S \approx 0.21$ at 1.4 W to $T_{xx}^S \approx 0.40$, whereas the component $T_{zz}^S \approx 0.13$ remains relatively constant [40]. Most important, all the diagonal elements T_{xx}^S , T_{yy}^S , and T_{zz}^S are clearly larger than zero. This demonstrates that there is a directed transfer of information from the upper to the lower particle (otherwise T^S would be smaller than zero). Hence, this supports that the interaction between upper and lower particle can be described by a nonreciprocal interaction where the upper particle forms the ion focus and the lower reacts to this ion focus without reaction of the upper particle.

To study the effects of the plasma properties on the STE such two-particle systems have been studied under different rf powers and gas pressures. Also, the thermophoretic force to levitate the particles against gravity has been varied. This allows us to trap the two particles at different heights in the plasma sheath and at different vertical interparticle distances in order to judge the influence of the ion focus strength on the STE. The results of this survey are shown in Fig. 2 for the directionality index T_{xx}^S using the x coordinates of upper and lower particle, only. Since no clear trend for the behavior of T_{xx}^S is seen as a function of rf power or gas pressure, the directionality index is given as a function of vertical interparticle distance in Fig. 2(a) and height above the electrode in Fig. 2(b). There clearly the information transfer increases with decreased interparticle distance. The gas pressure has only a little influence. This is understandable

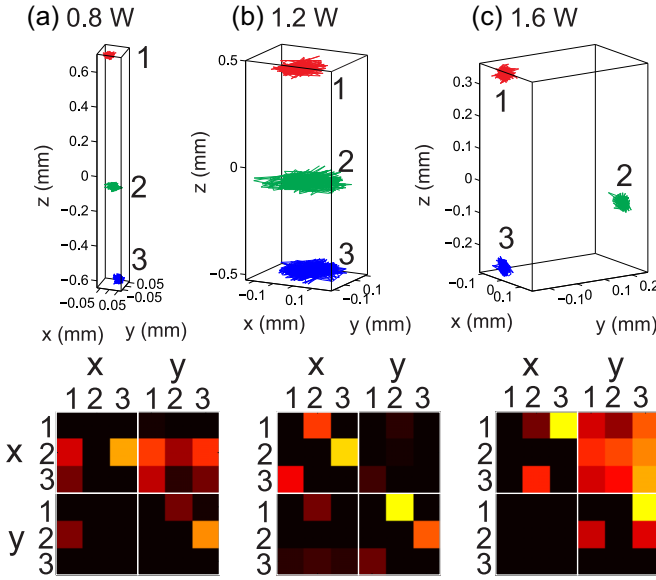


FIG. 3. (Color online) Particle trajectories of a three-particle system at discharge powers of (a) 0.8 W, (b) 1.2 W, and (c) 1.6 W at a gas pressure of 6 Pa together with the directionality index T_{xx}^S in false colors. The directionality index is calculated taking the x and y coordinates of the three particles against each other. The color bar is nearly the same as in Fig. 1.

since at closer vertical distance the influence of the ion focus of the upper particle becomes stronger. Further, with decreased height above the electrode the directionality index T_{xx}^S also increases, at least for gas pressures of 6 and 8 Pa; for the case of 4 Pa the trend is not that clear. This behavior is even reasonable, since, when at constant pressure the particles are located closer to the electrode, i.e., deeper in the sheath, the ion streaming motion can be assumed to increase, and the ion focus is then strengthened at least up to a certain streaming velocity of the order of the Bohm velocity [19,41]. Whether the somewhat different behavior of the measurements at a gas pressure of 4 Pa can be attributed to the fact that here already the ion focus strength decreases with increasing ion streaming velocity cannot be answered.

An interesting fact can be illustrated by the apparent outlier in Fig. 2(a) and 2(b), which is marked by the arrow. There the entropy transfer is found to be nearly vanishing. This data point corresponds to a very small interparticle distance of the order of 0.1 mm and a relatively small height above the electrode of only 15 mm. The peculiar trajectory of this particle pair is shown in Fig. 2 as an inset from which it is seen that here the upper particle moves in a circle whereas the lower is more or less stationary. In all other situations the particles are vertically aligned (as in Fig. 1). This indicates that the STE can serve as reliable indicator for determining vertically aligned situations with asymmetric interactions.

Extending these investigations, we will now study three-particle systems at different discharge powers; see Fig. 3. For the lower powers, we find three vertically aligned particles; for the highest discharge power, a triangular system is seen, where the uppermost and the lowermost particle are vertically aligned (particles 1 and 3). For these systems the directionality

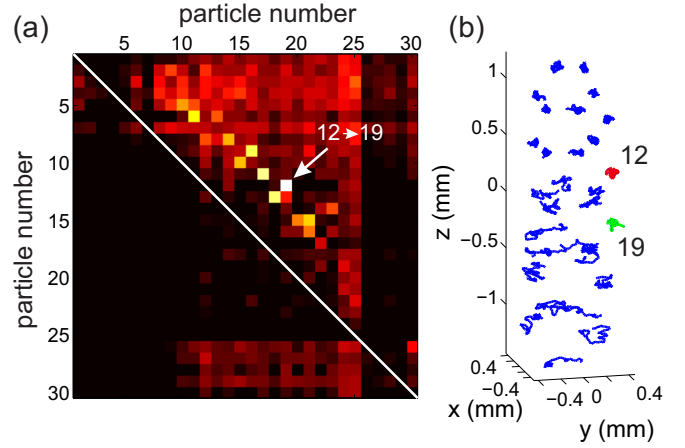


FIG. 4. (Color online) (a) Directionality index T_{xx}^S in false colors for a system with 30 particles (color bar as in Fig. 1). Here, the x -time series of all particles are calculated against each other. The particle number is counted from top to bottom. (b) Trajectories of the 30 particle system. See text for details.

index is calculated using the x and y coordinates of the particles against each other (obviously $T_{xx}^S = 0$ when using the same time series as input for A_i and B_i , hence the diagonal elements of the directionality matrix are exactly zero). Starting with the situation at 1.2 W [see Fig. 3(b)], one finds high positive values for T_{xx}^S at particle 1 influencing particle 2 (in both $x - x$ and $y - y$ coordinates), as well as particle 2 influencing particle 3 (in both $x - x$ and $y - y$ coordinates). So the information transfer is stepwise from the upper to the lower particle in this vertically aligned chain. The same behavior is seen for 0.8 W in Fig. 3(a), however, somewhat less pronounced. For the triangular case in Fig. 3(c) one finds the dominant contributions for entropy transfer from $1 \rightarrow 3$, but not for $1 \rightarrow 2$, again substantiating that the direct vertical interaction is decisive. This is in perfect agreement with an analysis using (instantaneous) normal modes under the influence of an ion focus [22].

Finally (see Fig. 4) in an even larger system of 30 particles, the directionality index T_{xx}^S is determined for the $x - x$ interaction of all particles against each other (also here the diagonal elements are zero). The particles are counted here from top to bottom along their (vertical) z coordinate. It is now seen that almost only the upper triangular part of the directionality matrix shows positive values. This clearly indicates that the information flow is from top to bottom (since the particle count is also arranged this way). As an example, the maximum value for the STE is found for particle 12 influencing particle 19 (marked by the arrow). Now, these two particles are also highlighted in the trajectories of the 30-particle cluster in Fig. 4(b), and they are found to be vertically aligned and positioned just atop of each other substantiating that the STE serves as a powerful indicator of vertical alignment.

To summarize, we have demonstrated that the symbolic transfer entropy that has been used for statistical interpretation of information transport from a driving to a responding agent in other systems can be successfully applied to the asymmetry introduced by the ion focus (wakefield) interaction

in dusty plasmas. The STE reveals that indeed information is transported from an upper particle in an ion flow to a lower. The information transfer increases with decreased interparticle distance and trapping height in the plasma sheath, which can be reasonably explained by the ion flow and its role in the formation of the ion focus. This technique is also reliably applicable to larger particle clusters and will open up new

directions for the statistical interpretation of the asymmetric interactions in dusty plasmas.

We gratefully acknowledge financial support from DFG under grant no. SFB-TR24, project A3 and from the Helmholtz-Gemeinschaft via HEPP. We like to thank B. Pompe (University Greifswald) for helpful discussions.

-
- [1] A. Ivlev, H. Löwen, G. Morfill, and C. P. Royall, *Complex Plasmas and Colloidal Dispersions: Particle-Resolved Studies of Classical liquids and Solids*, Series in Soft Condensed Matter 5 (World Scientific, Singapore, 2012).
 - [2] A. Piel, *Plasma Physics: An Introduction to Laboratory, Space, and Fusion Plasmas* (Springer, Heidelberg, 2010).
 - [3] P. K. Shukla and A. A. Mamun, *Introduction to Dusty Plasma Physics* (Institute of Physics Publishing, Bristol, 2002).
 - [4] D. Block and A. Melzer, in *Introduction to Complex Plasmas*, Springer Series on Atomic, Optical, and Plasma Physics, edited by M. Bonitz, N. Horing, and P. Ludwig (Springer, New York, 2010), pp. 135–154.
 - [5] S. V. Vladimirov and M. Nambu, *Phys. Rev. E* **52**, R2172 (1995).
 - [6] M. Nambu, S. V. Vladimirov, and P. K. Shukla, *Phys. Lett. A* **203**, 40 (1995).
 - [7] V. A. Schweigert and M. S. Obrekht, *Pisma Zhur. Tech. Fis.* **21**, 57 (1995) [*Tech. Phys. Lett.* **21**, 377 (1995)].
 - [8] A. Melzer, V. A. Schweigert, I. V. Schweigert, A. Homann, S. Peters, and A. Piel, *Phys. Rev. E* **54**, R46 (1996).
 - [9] K. Takahashi, T. Oishi, K.-i. Shimomai, Y. Hayashi, and S. Nishino, *Phys. Rev. E* **58**, 7805 (1998).
 - [10] G. A. Hebner, M. E. Riley, and B. M. Marder, *Phys. Rev. E* **68**, 016403 (2003).
 - [11] A. A. Samarian, S. V. Vladimirov, and B. James, *JETP Lett.* **82**, 758 (2005).
 - [12] S. K. Zhdanov, A. V. Ivlev, and G. E. Morfill, *Phys. Plasmas* **16**, 083706 (2009).
 - [13] L. Couëdel, S. K. Zhdanov, A. V. Ivlev, V. Nosenko, H. M. Thomas, and G. E. Morfill, *Phys. Plasmas* **18**, 083707 (2011).
 - [14] L. Couëdel, V. Nosenko, A. V. Ivlev, S. K. Zhdanov, H. M. Thomas, and G. E. Morfill, *Phys. Rev. Lett.* **104**, 195001 (2010).
 - [15] B. Liu, J. Goree, and Y. Feng, *Phys. Rev. Lett.* **105**, 085004 (2010).
 - [16] M. Kroll, J. Schablinski, D. Block, and A. Piel, *Phys. Plasmas* **17**, 013702 (2010).
 - [17] I. H. Hutchinson, *Phys. Rev. Lett.* **107**, 095001 (2011).
 - [18] I. H. Hutchinson, *Phys. Rev. E* **85**, 066409 (2012).
 - [19] P. Ludwig, W. J. Miloch, H. Kählert, and M. Bonitz, *New J. Phys.* **14**, 053016 (2012).
 - [20] T. B. Röcker, A. V. Ivlev, R. Kompaneets, and G. E. Morfill, *Phys. Plasmas* **19**, 033708 (2012).
 - [21] K. Qiao, J. Kong, E. V. Oeveren, L. S. Matthews, and T. W. Hyde, *Phys. Rev. E* **88**, 043103 (2013).
 - [22] A. Melzer, A. Schella, and M. Mulsow, *Phys. Rev. E* **89**, 013109 (2014).
 - [23] V. A. Schweigert, I. V. Schweigert, A. Melzer, A. Homann, and A. Piel, *Phys. Rev. E* **54**, 4155 (1996).
 - [24] A. Melzer, V. A. Schweigert, and A. Piel, *Phys. Rev. Lett.* **83**, 3194 (1999).
 - [25] A. Melzer, V. Schweigert, and A. Piel, *Phys. Scr.* **61**, 494 (2000).
 - [26] A. A. Samarian, S. V. Vladimirov, and B. W. James, *Phys. Plasmas* **12**, 022103 (2005).
 - [27] V. R. Ikkurthi, K. Matyash, A. Melzer, and R. Schneider, *Phys. Plasmas* **17**, 103712 (2010).
 - [28] W. J. Miloch, M. Kroll, and D. Block, *Phys. Plasmas* **17**, 103703 (2010).
 - [29] J. Carstensen, F. Greiner, D. Block, J. Schablinski, W. J. Miloch, and A. Piel, *Phys. Plasmas* **19**, 033702 (2012).
 - [30] A. Kaiser and T. Schreiber, *Physica D* **166**, 43 (2002).
 - [31] P. F. Verdes, *Phys. Rev. E* **72**, 026222 (2005).
 - [32] P.-O. Amblard and O. J. J. Michel, *Entropy* **15**, 113 (2012).
 - [33] M. Staniek and K. Lehnertz, *Phys. Rev. Lett.* **100**, 158101 (2008).
 - [34] C. Bandt and B. Pompe, *Phys. Rev. Lett.* **88**, 174102 (2002).
 - [35] We have used $m = 3$ and $\ell = 5$ in the calculations presented here. Other choices of m and ℓ show the same qualitative behavior. The STE is calculated as the average over subdividing the time series into sequences of 1000 data points.
 - [36] O. Arp, D. Block, A. Piel, and A. Melzer, *Phys. Rev. Lett.* **93**, 165004 (2004).
 - [37] S. Käding, D. Block, A. Melzer, A. Piel, H. Kählert, P. Ludwig, and M. Bonitz, *Phys. Plasmas* **15**, 073710 (2008).
 - [38] A. Schella, T. Miksch, A. Melzer, J. Schablinski, D. Block, A. Piel, H. Thomsen, P. Ludwig, and M. Bonitz, *Phys. Rev. E* **84**, 056402 (2011).
 - [39] O. Arp, D. Block, M. Klindworth, and A. Piel, *Phys. Plasmas* **12**, 122102 (2005).
 - [40] Since the base-2-logarithm is used in Eq. (1) the values can be interpreted as information gain in bits. However, the absolute values depend on the particular choice of m and ℓ .
 - [41] D. Block, J. Carstensen, P. Ludwig, W. Miloch, F. Greiner, A. Piel, M. Bonitz, and A. Melzer, *Contrib. Plasma Phys.* **52**, 804 (2012).